

Structural relaxations in glass forming poly(butadiene): A molecular dynamics study

A. van Zon and S. W. de Leeuw

Department of Applied Physics, Delft University of Technology, Lorentzweg 1, 2628 CJ Delft, The Netherlands

(Received 16 March 1998)

We present results of a molecular dynamics simulation of a realistic model of poly(butadiene). We find Rouse-like dynamics and the corresponding diffusion coefficient shows a power law behavior. The coherent intermediate scattering functions clearly show a crossover from Debye to non-Debye relaxation. The latter can be described accurately by a stretched exponent. It is shown that the second scaling law of the mode-coupling theory is valid for $k=1.60$ and 2.40 \AA^{-1} in the temperature range measured. The corresponding relaxation times also follow the temperature dependence of the mode-coupling theory. [S1063-651X(98)51110-5]

PACS number(s): 64.70.Pf, 61.25.Hq, 61.20.Ja

In past decades the dynamical behavior of glass forming materials has been a subject of wide interest. The main ideas of the dynamics, just above the structural glass transition, are based on the mode-coupling theory (MCT). Originally introduced to describe the dynamics of dense liquids, it was applied by Leutheusser to describe the structural arrest near the glass transition [1]. In later years MCT has been extended, which has led to important scaling laws for structural relaxations in undercooled liquids [2]. In the case of simple monatomic liquids, molecular dynamics simulations have provided much information about the dynamical properties of ‘‘normal’’ and undercooled liquids [3,4]. Unfortunately, the results of these simulations are rarely compared with experiments. This is because of the extremely high cooling rate needed to avoid crystallization in simple liquids. Therefore, experimental results are usually obtained from ‘‘good’’ glass formers, for example, polymers. A polymer that is extensively studied using neutron scattering is poly(butadiene) (PB) [5]. The results of these neutron scattering experiments are difficult to interpret and they only give limited information about the dynamics. Here, as in the case of simple liquids, molecular dynamics simulations can provide detailed information about the dynamics of glass forming polymers. Most molecular dynamics simulations of polymers are performed at temperatures well above the glass transition and the results are analyzed within the framework of Rouse-like dynamics [6,7]. In other cases, no connection with MCT is made [8]. However, Monte Carlo (MC) simulations showed that MCT can be applied to polymers but to what extent is still unclear [9,10]. The simulations we performed are different from others because we have used a realistic model of a polymer with fixed bond length. This is in contrast to the well-known bead-spring model. We determined the coherent intermediate scattering function, which can be compared directly with neutron scattering experiments. The results are analyzed both phenomenologically and within the framework of MCT.

In our simulations a united atom model of 1,4-poly(butadiene) ($-\text{CH}_2-\text{CH}=\text{CH}-\text{CH}_2-$) $_n$ is used. The distances between two connected carbon atoms are 1.43 \AA for the CH_3-CH and CH_2-CH bonds, 1.33 \AA for the $\text{CH}=\text{CH}$ bond, and 1.53 \AA for the CH_2-CH_2 bond. These values are fixed during the simulation. The general form of valence and torsion potentials is shown in Eqs. (1) and (2)

[11]. For the nonbonded interaction, a Lennard-Jones potential is used, which is shown in Eq. (3)

$$V_{\text{bend}}(\theta) = \frac{k_\theta}{2} (\cos \theta - \cos \theta_0)^2, \quad (1)$$

$$V_{\text{tors}}(\phi) = \sum_{n=1}^6 a_n \cos^n \phi, \quad (2)$$

$$V_{LJ}(r) = 4 \epsilon \left[\left(\frac{\sigma}{r} \right)^{12} - \left(\frac{\sigma}{r} \right)^6 \right]. \quad (3)$$

Here θ is the bond and ϕ the torsion angle, and k_θ is related to the small angle force constant k via $k_\theta = k/\sin^2 \theta_0$. Numerical details of these potentials can be found in Ref. [11].

Starting configurations are made using a pivot Monte Carlo algorithm with a Metropolis acceptance criterion [12]. In this way, 24 chains of 100 carbon atoms (=25 monomers) are made. 100 000 pivot moves per chain are performed in order to avoid correlation between the chains. After this, the 24 polymers are brought together in a computational box (cube) with a size of 39 \AA^3 leading to a density of 0.89 g/cm^3 [13]. Excluded volume is gradually ‘‘switched on’’ using a truncated Lennard-Jones potential. Finally, the system is equilibrated for 4 ns with molecular dynamics. In these simulations the bond lengths between the carbon atoms are kept fixed using constraint dynamics [14]. The temperature is regulated via a Nosé-Hoover thermostat [15].

Near the glass transition temperature T_g , structural arrest reduces the number of degrees of freedom contributing to, e.g., the specific heat or the compressibility. Empirically, the glass transition temperature is determined by measuring the energy of the system as a function of the temperature, or the volume as a function of the pressure. A result of this measurement for PB is shown in Fig. 1. Here, the system is cooled from $T=0.5$, which corresponds to 451 K, in steps of 0.025, and is equilibrated at each temperature for 40 ps. The straight lines correspond to a linear fit with slopes of 1.99 and $2.38 \text{ kJ}/(\text{mol K})$ below and above T_g . The change in the slope is small but clearly visible at $T=0.15$, corresponding to a temperature of 135 K. This is well below the glass transition temperature of 186 K measured in experiments [5].

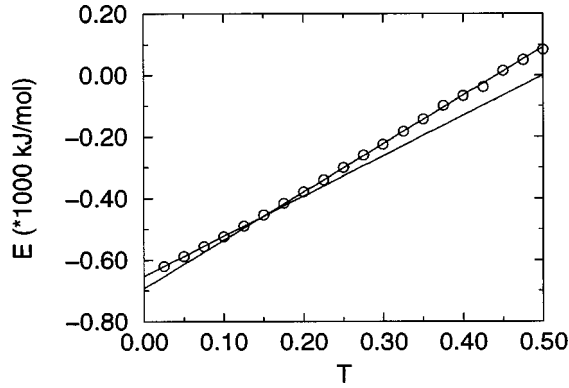


FIG. 1. Temperature dependence of the energy obtained from stepwise cooling. The glass transition temperature is estimated at $T=0.15$. The straight lines correspond to a linear fit with slopes of 1.99 and 2.38 kJ/(mol K) below and above T_g .

This is probably caused by the length of the polymer chains, which is small compared to the length of the chains used in experiments [16]. Note that the cooling rate is extremely high, which usually leads to a higher T_g value.

To analyze the glass transition dynamics we determined the mean square displacement of the carbon atoms. The results are shown in Fig. 2. The “diffusion” coefficient is determined using

$$\langle R^2(t) \rangle = (Dt)^\alpha \quad (4)$$

in the long time limit. As shown in Fig. 2, $\alpha=0.62$, which is somewhat higher than the 0.5 of ideal Rouse dynamics and close to the 0.67 of Zimm dynamics [17]. No crossover to a linear time dependence is found on this time scale. The temperature dependence of D is shown in the inset of Fig. 2. The straight line is a fit according to a power law:

$$D(T) \sim (T - T_c)^\gamma, \quad (5)$$

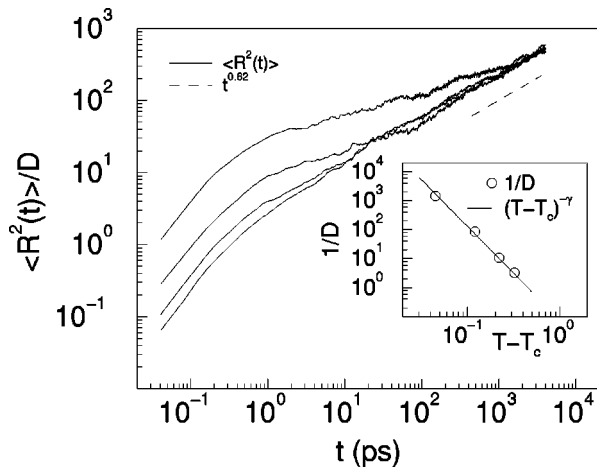


FIG. 2. Mean square displacement of the C atoms at four different temperatures: $T=0.5$, $T=0.4$, $T=0.3$, and $T=0.225$. Inset: temperature dependence of the diffusion coefficient defined in Eq. (4). The straight line is a fit according to Eq. (5), with $T_c=0.18$ and $\gamma_{kww}=3.2$.

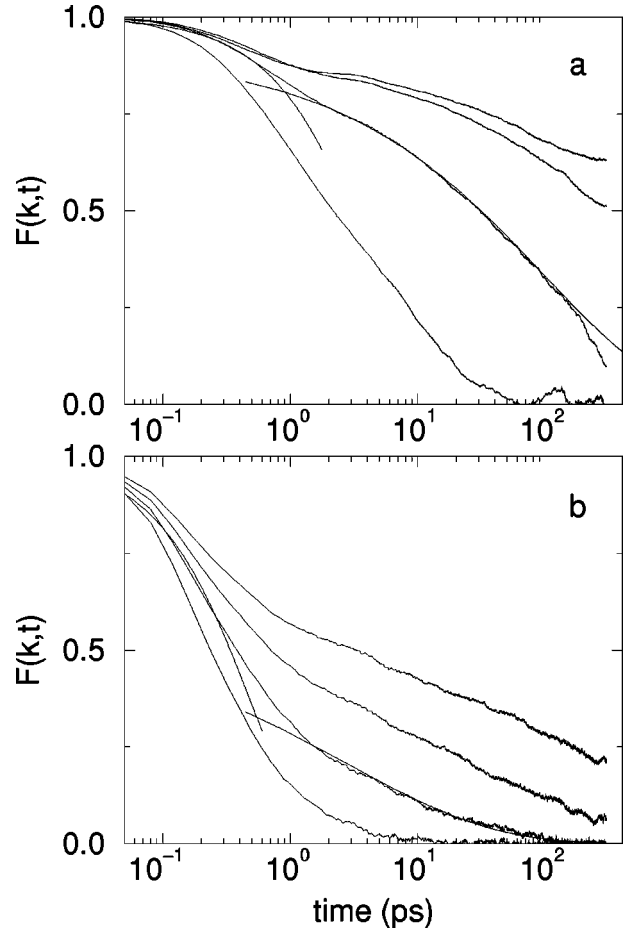


FIG. 3. Coherent intermediate scattering function for $k=1.60 \text{ \AA}^{-1}$ (a) and $k=2.40 \text{ \AA}^{-1}$ (b) at four different temperatures: $T=0.225$, $T=0.25$, $T=0.30$, and $T=0.40$ (top to bottom). Representative fits according to Eqs. (7) and (8), are also shown. The β 's found in this way are 0.45 for $k=1.60 \text{ \AA}^{-1}$ and 0.37 for $k=2.40 \text{ \AA}^{-1}$.

with $T_c=0.18$, consistent with $T_g=0.15$ and $\gamma=3.2$. This value of γ is much larger than corresponding values obtained in simulations of simple liquids [4].

Another important quantity in analyzing the glass transition dynamics is the intermediate scattering function $F(k,t)$ given in Eq. (6) [18]:

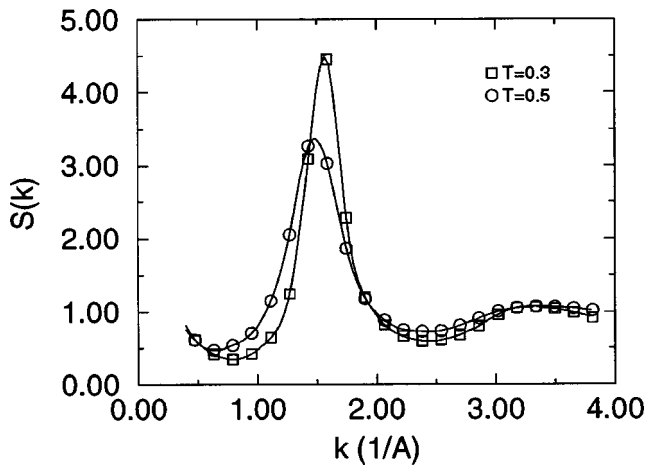
$$F(k,t) = \left\langle \sum_i \sum_j e^{-i\mathbf{k} \cdot [\mathbf{r}_i(t) - \mathbf{r}_j(0)]} \right\rangle. \quad (6)$$

To make a connection with experiments, we determined the coherent part of $F(k,t)$. For a phenomenological interpretation, $F(k,t)$ can be split into two regions:

$$F(k,t) \sim e^{-t/\tau_D}, \quad t < t_c, \quad (7)$$

$$F(k,t) \sim e^{-(t/\tau_{kww})^\beta}, \quad t > t_c, \quad (8)$$

where t_c is the crossover time, which can be temperature and k dependent. The nature of this crossover and the relation to the glass transition is still unclear. One explanation is that the stretched exponential behavior is caused by a crossover from vibrational to relaxational motion, the vibration-relaxation model [5]. In this way the vibrational and relaxational mo-


 FIG. 4. Static structure factor $S(k)$ at $T=0.5$ and $T=0.3$.

tion are related to β - and α -relaxation, respectively. Another explanation is that this behavior is caused by the crossover from independent to cooperative dynamics of the chain segments, and is therefore a property of polymer dynamics and not directly related to the glass transition [19]. This can be understood by using the Gaussian approximation of the incoherent intermediate scattering function in which α in Eq.

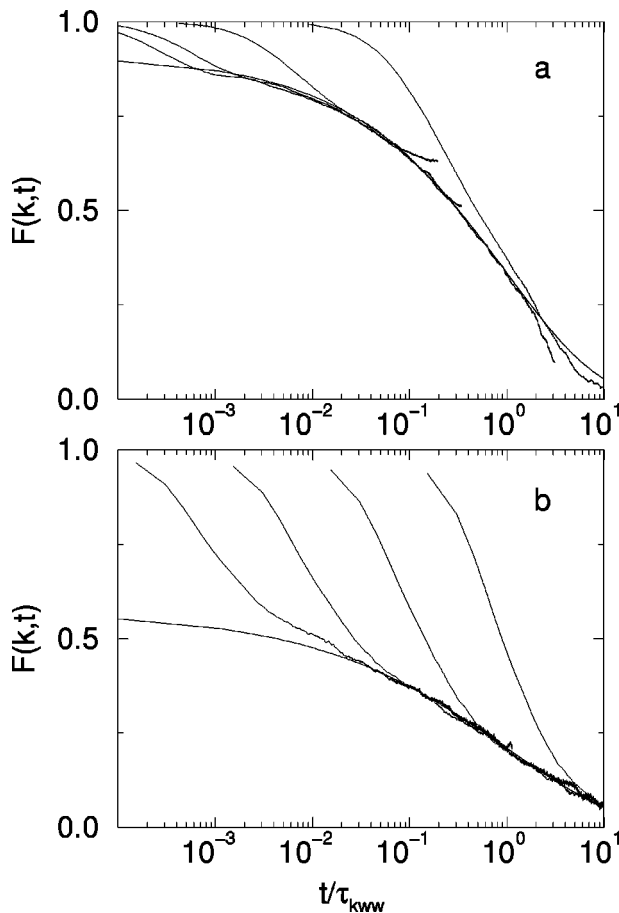


FIG. 5. Rescaled coherent intermediate scattering function for $k=1.60 \text{ \AA}^{-1}$ (a) and $k=2.40 \text{ \AA}^{-1}$ (b) at four different temperatures, $T=0.225$, $T=0.25$, $T=0.30$, and $T=0.40$ (left to right). The master function $\tilde{F}(k,t)$, which is Eq. (8), with $\tau_{kww}=1$, is also shown.

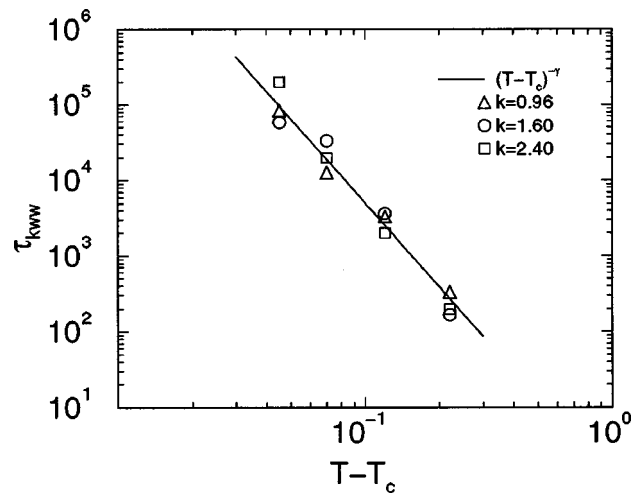


FIG. 6. τ_{kww} for $k=0.96 \text{ \AA}^{-1}$, $k=1.60 \text{ \AA}^{-1}$, and $k=2.40 \text{ \AA}^{-1}$ at four different temperatures: $T=0.225$, $T=0.25$, $T=0.30$, and $T=0.40$. The solid line is fit according to Eq. (5), with $T_c=0.18$ and $\gamma_{kww}=3.7$.

(4) and β in Eq. (8) are identical. In Fig. 3 the results of a measurement of $F(k,t)$ are shown for $k=1.60 \text{ \AA}^{-1}$ (a) and $k=2.40 \text{ \AA}^{-1}$ (b) at four different temperatures: $T=0.225$, $T=0.25$, $T=0.30$, and $T=0.40$ (top to bottom). The values of $F(k,0)$ are normalized to unity; the normalization constant $S(k)$ is the static structure factor and is shown in Fig. 4. The first peak of $S(k)$ corresponds to the intermolecular distance and is temperature dependent. The second peak corresponds to the intramolecular distance and is therefore temperature independent. $k=1.60 \text{ \AA}^{-1}$ and $k=2.40 \text{ \AA}^{-1}$ correspond, respectively, to the first peak and the first minimum of $S(k)$. At these k values a representative fit according to Eqs. (7) and (8) is shown. The crossover is clearly visible at all temperatures and both k values and t_c is approximately 1 ps. This crossover is also seen in the incoherent scattering functions, which are not shown here.

One of the important results of the MCT is the second scaling law [2], which states that in the time regime of the α relaxation a master function $\tilde{F}(k,t)$ exists such that

$$F(k,t,T) = \tilde{F}(k,t/\tau(T)). \quad (9)$$

This is also referred to as the time-temperature superposition principle. In our case, $\tau(T)$ in Eq. (9) corresponds to τ_{kww} in Eq. (8). When this τ_{kww} is determined one can rescale $F(k,t)$. The result of this is shown in Fig. 5 for the same k and T values as in Fig. 3. The master function $\tilde{F}(k,t)$, which is Eq. (8) with $\tau_{kww}=1$, is also shown. It is clear that the second scaling law, Eq. (9), is valid for both k values in this temperature range. The β 's found in this way are 0.45 for $k=1.60 \text{ \AA}^{-1}$ and 0.37 for $k=2.40 \text{ \AA}^{-1}$. This is in good agreement with experimental results obtained by neutron scattering (also 0.45 and 0.37) [20]. The difference between these values and the 0.62 of the Gaussian approximation can be explained by α -relaxation stretching [2]. The k dependence of β is caused by the k dependence of $S(k)$. This is included in extended versions of MCT, which can only be solved numerically [2]. A detailed analysis of this k dependence will be described in a future publication.

According to MCT, τ_{kww} follows the same temperature dependence as the diffusion coefficient. This temperature dependence is shown in Fig. 6 for $k=0.96, 1.60,$ and 2.40 \AA^{-1} . The straight line is a fit according to Eq. (5) with $T_c=0.18$ and $\gamma_{kww}=3.7$. No k dependence of γ_{kww} is observed. The value of γ_{kww} is similar to γ_D and values obtained by MC simulations [9]. Since the α relaxation takes place in the Rouse regime, it is influenced by the relaxations in the chain. However, this cannot explain the high values of γ_D and γ_{kww} . Recently, Bennemann *et al.* performed a molecular dynamics simulation of polymers in which smaller values of γ were observed. This is probably caused by the smaller chain length of only 10 beads [21].

In summary, we have performed a molecular dynamics simulation of a realistic model of poly(butadiene). The coherent intermediate scattering function was calculated and

analyzed in the framework of MCT. It is shown that in the temperature range measured, the second scaling law is valid for $k=1.60$ and 2.40 \AA^{-1} . The β 's found in this way, 0.45 and 0.37, are in agreement with experimental results. The temperature dependence of the α relaxation, which takes place in the Rouse regime, and the diffusion coefficient, follow the predictions of MCT. A full analysis within the framework of MCT, for both coherent and incoherent intermediate scattering functions, will be described in a future publication.

This work is part of the research program of the Foundation for Chemical Research (SON) and was made possible by financial support from the Netherlands Organization for Scientific Research (NWO). We thank the Center for High Performance Applied Computing (HPaC) for a generous allocation of computing time on the CRAY-T3E.

-
- [1] E. Leutheusser, *Phys. Rev. A* **29**, 2765 (1984).
 [2] See W. Götze, in *Liquids, Freezing and the Glass transition*, edited by J. P. Hansen, D. Levesque, and J. Zinn-Justin (North-Holland, Amsterdam, 1990).
 [3] J. Ullo and Sindney Yip, *Phys. Rev. A* **39**, 5877 (1989).
 [4] M. J. D. Brakkee and S. W. de Leeuw, *J. Phys.: Condens. Matter* **2**, 4991 (1990).
 [5] See, e.g., R. Zorn, A. Arbe, J. Colmenero, B. Frick, D. Richter, and U. Buchenau, *Phys. Rev. E* **52**, 781 (1995).
 [6] Kurt Kremer and Gary S. Grest, *J. Chem. Phys.* **92**, 5057 (1990).
 [7] A. Kopf, B. Dünweg, and W. Paul, *J. Chem. Phys.* **107**, 6945 (1997).
 [8] Ryong-Joon Roe, *J. Chem. Phys.* **100**, 1610 (1994).
 [9] Jörg Baschnagel, *Phys. Rev. B* **49**, 135 (1994).
 [10] For a review on simulations in polymer science, see *Monte Carlo and Molecular Dynamics Simulations in Polymer Science*, edited by K. Binder (Oxford University Press, New York, 1995).
 [11] Stephen L. Mayo, Barry D. Olafson, and William A. Goddard III, *J. Phys. Chem.* **94**, 8897 (1990).
 [12] Sylvie Neyertz and David Brown, *J. Chem. Phys.* **102**, 9725 (1995).
 [13] D. W. van Krevelen and P. J. Hoftyzer, *Properties of Polymers—Their Estimation and Correlation with Chemical Structure* (Elsevier Scientific Publishing Company, Amsterdam, 1976).
 [14] S. W. de Leeuw, J. W. Perram, and H. G. Petersen, *J. Stat. Phys.* **61**, 1203 (1990).
 [15] William G. Hoover, *Phys. Rev. A* **31**, 1695 (1985).
 [16] See R.-J. Roe, in *Advances in Polymer Science 116*, edited by L. Monnerie and U. W. Suter (Springer-Verlag, Berlin, 1994).
 [17] M. Doi and S. F. Edwards, *The Theory of Polymer Dynamics* (Clarendon Press, Oxford, 1986).
 [18] J. P. Hansen and I. R. McDonald, *Theory of Simple Liquids* (Academic Press, New York, 1986).
 [19] J. Colmenero, A. Arbe, G. Coddens, C. Mijangos, and H. Reinecke, *Phys. Rev. Lett.* **78**, 1928 (1997).
 [20] For $\beta=0.45$, see D. Richter, B. Frick, and B. Farago, *Phys. Rev. Lett.* **61**, 2465 (1988); for $\beta=0.37$, see D. Richter, R. Zorn, B. Farago, B. Frick, and L. J. Fetters, *ibid.* **68**, 71 (1992).
 [21] Christoph Bennemann, Wolfgang Paul, Kurt Binder, and Burkhard Dünweg, *Phys. Rev. E* **57**, 834 (1998).